Research in Veterinary Science 89 (2010) 332–339

Contents lists available at ScienceDirect

Research in Veterinary Science

journal homepage: www.elsevier.com/locate/rvsc

Cytokine profiles, apoptosis and pathology of experimental *Pasteurella multocida* serotype A1 infection in mice

P. Ezhil Praveena [a], Sivakumar Periasamy [a,*], A.A. Kumar [b], Nem Singh [a]

[a] Division of Veterinary Pathology, Indian Veterinary Research Institute, Izatnagar 243 112, India
[b] Division of Bacteriology, Indian Veterinary Research Institute, Izatnagar 243 112, India

ARTICLE INFO

Article history:
Accepted 13 April 2010

Keywords:
Apoptosis
Cytokines
Mice
Pathology
Pasteurella multocida

ABSTRACT

Mice were experimentally infected with *Pasteurella multocida* serotype A1 to study the cytokine profiles, host cell apoptosis and sequential pathology at different hours of post-infection. Infected mice were dull, anorectic and depressed. A transient leukocytopenia followed by progressive leukocytosis was observed in the course of infection. Serum cytokine profiles showed significantly ($P < 0.01$) higher amount of pro-inflammatory cytokines (TNF-α, IL-1β, IL-6 and mouse KC) in the infected mice when compared to control mice. The circulating lymphocytes were apoptotic on annexin V staining. Apoptotic nuclei were detected in splenocytes, hepatocytes and infiltrating leukocytes of the lungs on TUNEL staining. The lungs were grossly congested and hemorrhagic, and showed infiltration with polymorphonuclear cells at early and mononuclear cells in the late hours of infection. Alveolar epithelia, inter-alveolar septa and capillary endothelium of the lungs showed ultrastructural changes. Liver had degenerative changes in histological and ultrathin sections.

Published by Elsevier Ltd.

1. Introduction

Pasteurella multocida is a Gram-negative bacterium causing variety of diseases in mammals and birds. *P. multocida* serogroup A is one of the nasopharyngeal commensal pathogens associated with respiratory diseases in animals. Despite continuing investigations for several decades, the mechanisms by which the isolates of *P. multocida* incite rapid pathogenesis and acute clinical diseases are poorly understood. The bacterial components such as capsular or outer membrane proteins and endotoxins have been reported as virulence factors responsible for immuno-pathological changes (Boyce and Adler, 2006; Fuller et al., 2000; Hodgson, 2006; Ryu and Kim, 2000), but there is limited information on host factors that play a role in disease pathogenesis in the milieu of host-pathogen interactions. The immuno-pathological changes of endotoxin-producing bacterial infections represent an uncontrolled over-reaction by the host immune system to the endotoxins (Hodgson, 2006; Morrison et al., 1999). This over-reaction takes the form of cascade events, which are mediated by pro-inflammatory cytokines, chemokines and eicosanoids (Hodgson, 2006; Morrison et al., 1999; Yoshie et al., 2001). While these mediators drive the inflammatory reaction, they also aggravate tissue pathology in response to the bacterial components (Hodgson, 2006; Vogel and Hogen, 1990; Yoshie et al., 2001). In addition, bacterial proteins and endotoxins induce host cell apoptosis or cytolysis that results in loss of immunocompetent cells required for combating the infection (Hotchkiss et al., 1997; Stevens and Czuprynski, 1996; Wesche et al., 2005). To understand the pathogenesis of pasteurellosis, it is essential to investigate the profiles of host factors such as pro-inflammatory cytokines and chemokines that are produced in relation to the tissue pathology resulted at various time points of experimental infection. In the present study, we report the pro-inflammatory cytokine profiles, host cell apoptosis and pathology of mice experimentally infected with *P. multocida* serotype A1.

2. Materials and methods

2.1. Animals

Eight week-old Swiss Albino mice ($n = 160$) of either sex received from the Laboratory Animal Resource centre of the Institute were used in this study. Following 3–4 days of acclimatization period, animals were randomly divided into sixteen groups ($n = 10$ per group), based on their body weight and size and provided with sterilized food and water ad libitum. Animal care and the experimental procedures were carried out according to the recommendations and specified approval of the Institute Animal Ethics Committee under the guidelines set forth by the Committee for the Purpose of Control and Supervision of Experiments on Animals in India.

* Corresponding author. Tel.: +91 903 363 6648; fax: +91 903 877 5516.
E-mail address: sivakumar.periasamy@uthct.edu (S. Periasamy).

0034-5288/$ - see front matter Published by Elsevier Ltd.
doi:10.1016/j.rvsc.2010.04.012

2.2. Bacteria

P. multocida serotype A1 (P120) strain isolated from clinically infected cattle was used in the present study. The freeze-dried isolate was cultured in brain heart infusion (BHI) broth and blood agar medium containing 5% sheep blood. The pathogenicity of the isolate was tested in healthy mice by intraperitoneal inoculation of overnight culture, in which all of them were succumbed to infection between 24 and 36 h post-infection (PI). Bacteria re-isolated from these infected mice were used for preparation of bacterial inoculum. The specificity of the isolate was confirmed by growth characteristics on MacConkey agar, morphological characteristics on smears stained with Gram's iodine, and positive biochemical test for indole reaction. In addition, PCR and multiplex PCR specific for *P. multocida* serotype A were used to confirm the isolate (Gautam et al., 2004).

2.3. Preparation of bacterial inoculum

Bacterial colonies isolated from the heart blood of mice were cultured in BHI broth at 37 °C for overnight. From the overnight static culture, bacteria were sub-cultured for 3 h in shaking incubator at 37 °C. The bacterial cells were washed twice and re-suspended in sterile PBS. The bacterial density was measured using McFarland standards, and the bacterial inocula containing 10^8 CFU/ml were prepared. The number of CFU/ml of inoculum was calculated by spread-plate method in BHI agar plates.

2.4. Experimental infection and clinical observation

Of sixteen groups of mice, eight groups were inoculated with 0.2 ml of inoculum containing 10^8 CFU/ml bacteria and other eight groups with sterile PBS to serve as control for each infected groups. The intraperitoneal route was used in all the animals. Following infection, animals were closely observed for their activities, feed intake and demeanor (normal, dull or depressed), postural changes, and respiratory distress, if any. Of the infected groups, one group each was sacrificed at 6, 12, 24, 36, 48, 60, 72 and 96 h PI. One uninfected control group was sacrificed to each time point of infected groups. All the animals were sacrificed by cervical dislocation.

2.5. Collection of blood and serum

Blood was collected from all animals just prior to sacrifice, either by venupuncturing at tail or cardiocentesis. About 0.2 ml blood was collected in sterile microcentrifuge tube containing EDTA (1 mg/ml) for hematological and apoptotic assays, and up to 0.5 ml without anticoagulant for serum separation. The hematobiochemical estimations were performed using standard procedures as described previously (Praveena et al., 2007). Serum samples were processed freshly for biochemical assays or stored frozen at −80 °C for cytokine assays. Serum was collected in additional time points at 12, 24 and 48 h PI from the groups sacrificed at 60, 72 and 96 h, respectively, for cytokine assays.

2.6. Flow cytometer detection of apoptosis in annexin V^{FITC}/PI stained lymphocytes

Apoptosis of circulating lymphocytes were detected by annexin V^{FITC}/propidium iodide (PI) staining kit (Sigma, MO, USA) following the manufacturer's instructions. From the whole blood, erythrocytes were removed by RBC lysis buffer and leukocytes were stained with annexin V^{FITC}/PI. Following incubation at room temperature for 10 min in the dark, the cells were analyzed on BD FACScalibur. A total of 10,000 gated lymphocytes from each sample were analyzed and the percentages of apoptotic cells were calculated using CellQuest Pro™ software. In addition, the annexin V^{FITC}/PI stained cells were counted to a total of 300 cells under fluorescence microscope in five randomly selected fields. The apoptotic index was calculated by dividing the total number of apoptotic cells with total number of cells counted.

2.7. Serum cytokine profile analysis

Using commercially available cytokine ELISA kits, the protein concentrations of pro-inflammatory cytokines such as IL-1β, TNF-α and IL-6 (Endogen, IL, USA), and mouse KC (R&D Systems, MN, USA) were determined in three pooled (three animals per pool) sera samples of both infected and uninfected control mice sacrificed at each time points.

IL-1β, TNF-α, IL-6 assays: The assays were carried out following the procedures of manufacturer's instructions. Briefly, 50 μl of recombinant-cytokine standard and test sera (including infected and control groups) were added to the duplicate wells pre-coated with monoclonal anti-mouse IL-1β or TNF-α or IL-6 antibodies, followed by 50 μl of biotinylated antibody reagent and incubated for 2 h. Following five washes, 100 μl of streptavidin-HRP conjugate was added to each well and incubated for 30 min. Following color development with 100 μl of TMB substrate, the absorbance was measured at 450 nm against the background absorbance at 550 nm. From the standard curves derived individually for IL-1β, TNF-α or IL-6 by plotting absorbance against the known concentrations of the recombinant cytokines, the level of these cytokines in serum samples were calculated.

Mouse KC assay: The mouse KC (homologue of IL-8 in other species) level was measured by using mouse KC quantification kit (R&D systems) following the manufacturer's procedures. Briefly, 50 μl of assay diluents was added to the wells pre-coated with monoclonal anti-mouse KC, and then 50 μl of standards or test sera (both control and infected groups) were added in duplicate wells, and incubated for 2 h at room temperature. Following four washes, 100 μl of conjugate was added to each well, incubated at room temperature for 2 h and color was developed in 30 min by adding substrate solution. The absorbance was measured at 450 nm against background absorbance at 550 nm. From the standard curve derived by plotting absorbance against the known concentration of the recombinant mouse KC, the concentrations in test serum samples were calculated.

2.8. Pathology

Following sacrifice of mice, necropsy was performed and visceral organs were examined for gross lesions. Heart blood was collected using sterile needle and streaked on blood agar for isolation of bacteria. Part of tissue samples collected from the lungs, liver, heart, kidney and spleen were preserved in 10% buffered neutral formalin for histopathology and remaining tissues were used for bacterial isolation and PCR. The formalin-fixed tissue samples were cut into pieces of 2–3 mm thickness and washed thoroughly with water and dehydrated in ascending grades of alcohol. The dehydrated tissues were embedded in paraffin blocks. Sections of 4 μm thickness were cut from paraffin blocks, and were routinely stained with haematoxylin and eosin (HE).

2.9. Immunoperoxidase test

Localization of bacterial antigens was performed in formalin-fixed tissues by immunoperoxidase staining procedure. Briefly, the tissue sections (lung, liver, kidney, spleen and heart) were heated in sodium citrate buffer (0.01 M, pH 6.0) to unmask the antigenic sites, and washed thrice in tris–borate saline (TBS, pH

7.4) containing high salt concentration (0.5 M). The endogenous peroxidase was blocked with 0.5% hydrogen peroxide for 30 min, and non-reactive sites with rabbit serum for 1 h at room temperature. Excess serum was drained off and anti-*P. multocida* A1 polyclonal hyperimmune serum raised in rabbit was added on the sections and incubated for overnight at 4 °C. Sections were washed thrice in TBS and incubated with anti-rabbit IgG peroxidase conjugate (Sigma, MO, USA) in 1:500 dilution for 1 h at 37 °C. The positive immunoreaction was identified with brown color development with freshly prepared diaminobenzidene tetrahydrochloride (DAB) in citrate buffer containing hydrogen peroxide and counterstained with Meyer's haematoxylin.

2.10. Transmission electron microscopy

Thin sections from the lungs and liver were fixed in 2.5% cold glutaraldehyde for 12 h, washed twice with cold PBS (0.2 M, pH 7.4) and treated with 1% osmium tetroxide for 4 h at 4 °C. The tissue pieces were dehydrated in ethyl alcohol, cleared and embedded in epon-araldite resin. Ultrathin sections were cut in ultramicrotome (Ultracut, Reichert-Jung, Austria), mounted onto copper grids and stained with uranyl acetate and subsequently with lead citrate. The sections were washed and dried on a filter paper in a covered petridishes. The grids were examined under electron microscope (Philips Morgagani 268).

2.11. In situ apoptosis detection by TUNEL procedure in tissues

Apoptotic changes on formalin-fixed tissues were detected *in situ* by Dead End Colorimetric TUNEL kit (Promega, Madison, USA) following the manufacturer's instructions. Briefly, tissue sections incubated with biotinylated nucleotide mixture were treated with streptavidin - HRP solution and immunoreaction was developed with DAB. The washed sections were mounted with glycerol and examined under the light microscope for apoptotic nuclei.

2.12. Bacterial culture

Bacterial isolation was done from heart blood, the lungs, liver and spleen. The heart blood collected in a sterile vial at the time of sacrifice was streaked onto blood agar medium and then subcultured in BHI broth. The pooled (three animals per pool) tissue samples were homogenized in sterile PBS and 100 μl of clear supernatant was plated in BHI agar and subsequently sub-cultured in BHI broth. The growth characteristics and biochemical properties of positive colonies were recorded and isolates were confirmed by PCR (Gautam et al., 2004).

2.13. Polymerase chain reaction (PCR) for bacterial genome detection

For bacterial genome detection by PCR, the DNA was isolated from pooled tissues (lung, liver, spleen and kidney) and bacterial culture using DNA isolation kit (MBI Fermentas, USA) following the manufacturers instructions. Using *P. multocida* serotype A1 specific primers (sense: 5′ AAT GTT TGC GAT AGT CCG TTA GA-3′ and anti-sense: 5′ ATT TGG CGC CAT ATC ACA GTC G-3′) flanking 540 bp length in the biosynthetic locus of *hyaC–hyaD* genes (Accession No. AF067175), the purified DNA was amplified for 30 cycles of denaturation at 94 °C for 30 s, annealing at 55 °C for 30 s, extension at 72 °C for 1 min. The amplified PCR products were electrophoresed in 1% agarose gel stained with ethidium bromide and visualized under UV trans-illuminator for size-specific bands. The specificity of PCR products was confirmed by restriction enzyme (RE) digestion with *Bgl*II, in which, two specific products, one at 410 bp and other at 130 bp were observed (Gautam et al., 2004).

2.14. Statistical analysis

Results are shown as mean ± standard error. For hematobiochemical, apoptosis and cytokine profile data that were normally distributed, comparisons between groups were performed by one-way ANOVA. The *P*-values < 0.05 were considered statistically significant.

3. Results

3.1. Clinical and hematobiochemical observations

Infected animals were dull and anorectic at early hours of infection (between 6 and 48 h PI). They showed mild crusting around eyes and nose, ruffled hairs and were reluctant to move. During the late hours of infection (between 60 and 96 h PI), animals were depressed, weak and huddled together. Two animals each at 24 and 36 h and one animal at 48 h PI were died due to septicemia. The animals in the control groups appeared normal. Among hematological parameters, the significant changes ($P < 0.05$) were observed in total and differential leukocyte counts. A transient leukocytopenia at 6–12 h and progressive leucocytosis at 24–60 h PI were observed. On differential leukocyte counts, neutrophilia followed by lymphocytopenia were observed. Among serum biochemical parameters, the levels of total protein and plasma fibrinogen were found to be increased (Praveena et al., 2007).

3.2. Detection of apoptosis in annexin V^{FITC}/PI stained circulating lymphocytes

The percentages of apoptosis in circulating lymphocytes at different h PI are represented in Fig. 1A. The base level apoptosis was found to be 0.8–1.4% in control animals. Among the infected groups, the apoptotic lymphocytes were higher at 36 (19.4 ± 3.6%) followed by 48 (18.4 ± 3.1%) and 24 (18 ± 3.0%) h PI, while they were lower at late hours of infection.

3.3. Bacterial isolation and PCR

The viable bacterial counts were estimated from the heart blood, spleen, liver and the lungs of the infected animals (Fig. 1B). Bacterial counts were higher in mice sacrificed at early hours than those mice sacrificed at late hours of infection. The average numbers of 1.4×10^5 CFU/ml of blood, 4×10^4 CFU/g spleen, 3×10^4 CFU/g of liver and 1×10^4 CFU/g lungs were recovered from mice sacrificed at 36 h PI, when compared to 3×10^3 CFU/ml of blood, 1.5×10^3 CFU/g of spleen, 8×10^2 CFU/g of lungs, and 6×10^2 CFU/g of liver at 96 h PI. Bacterial genome detection by PCR showed positive amplification of gene fragment specific for bacteria in the lungs, liver and spleen of the mice sacrificed between 12 and 60 h PI, whereas it was negative in other groups.

3.4. Serum cytokine profiles

The serum profiles of pro-inflammatory cytokines are represented in Fig. 2. Serum cytokine levels were significantly ($P < 0.01$) higher in the infected animals when compared to control animals. The level of TNF-α was found to be higher at 12 (0.15 ng/ml) and 24 (0.26 ng/ml) h PI (Fig. 2A). The level of IL-1β was found to be very high at 24 (0.63 ng/ml), 36 (0.623 ng/ml) and 48 (0.53 ng/ml) h PI (Fig. 2B). The profile of mouse KC followed similar trend as IL-1β and TNF-α with a higher concentration at 12 (0.6 ng/ml) and 24 (0.67 ng/ml) h PI (Fig. 2C). However, serum levels of these cytokines were found to be lower at late hours of infection. The

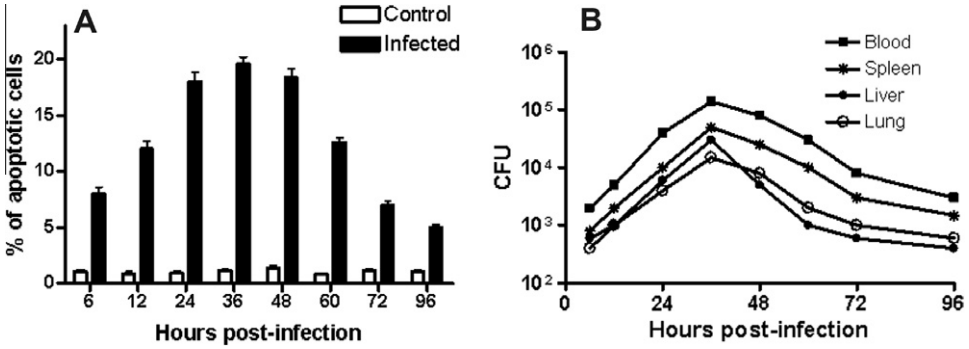

Fig. 1. (A) The circulating lymphocytes stained with annexin V/PI were analyzed in flow cytometer for apoptotic changes. The apoptotic indices at different time course of infection are represented in mean ± SE of four animals in each group. (B) Viable bacterial counts measured from heart blood, spleen, liver and the lungs of infected animals are shown as average number of CFU/ml of blood or gram of tissues from three pooled samples (three animals per pool) in each infected group.

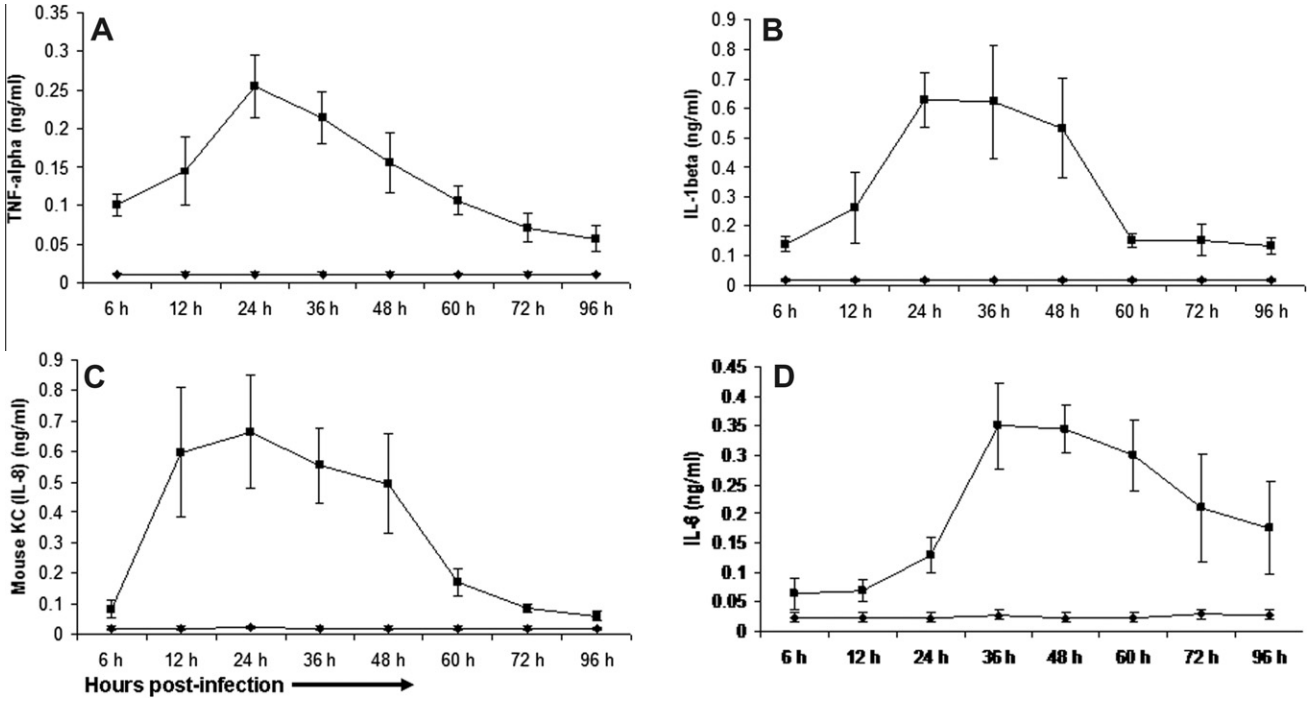

Fig. 2. The histograms showing the serum cytokine profiles of the infected (■) and control (∗) mice at different h PI. The serum levels of TNF-α (A), IL-1β (B), IL-8 (C) and IL-6 (D) are represented in mean ± SE of triplicate samples from three pooled sera samples (three animals per pool) for each infected and control groups.

concentration of IL-6 was found to be increased at 36 h PI (0.36 ng/ml) and remained higher until late hours of infection (Fig. 2D).

3.5. Pathology

Grossly the lungs were congested and hemorrhagic in animals sacrificed between 12 and 48 h PI, while mild congestion was observed in animals sacrificed at late h PI. No gross lesions could be observed in control group animals. Microscopically, the lungs showed infiltration with polymorphonuclear (PMN) cells in the alveolar space and engorged blood vessels in mice sacrificed between 12 and 48 h PI (Fig. 3). The bronchiolar lumen contained cellular exudates. Mice sacrificed between 60 and 96 h PI showed interstitial thickening, mononuclear cellular infiltration and hyperplastic bronchiolar epithelium. A seroproteinaceous exudation in the alveolar lumen and desquamation of bronchiolar epithelium were also observed. Liver showed degenerative changes such as intracytoplamic vacuolation, swollen nuclei and increased sinusoidal spaces at early h PI (Fig. 4), while engorged blood vessels and a few cellular infiltrates at late h PI. The lung and liver sections stained by immunoperoxidase procedure showed positive immunoreaction for the bacterial antigens in the infected animals, while it was absent in the tissue sections of control animals. The positive immunoreaction was observed as brown color spots in the alveolar space and liver sinusoidal spaces. Immunoreaction was intense (++) in mice sacrificed at 36 and 48 h PI, while it was less intense in other groups.

3.6. In situ detection of apoptosis by TUNEL staining

TUNEL staining showed round or crescent-shaped dark brown apoptotic nuclei in the lungs, liver and spleen. In the lungs, TUNEL-positive nuclei were seen in alveolar epithelial cells and infiltrating neutrophils and mononuclear cells (Fig. 5). In the liver, TUNEL-positive nuclei were seen in hepatocytes and infiltrating leukocytes at portal triads and mid-zonal areas. Spleen had more

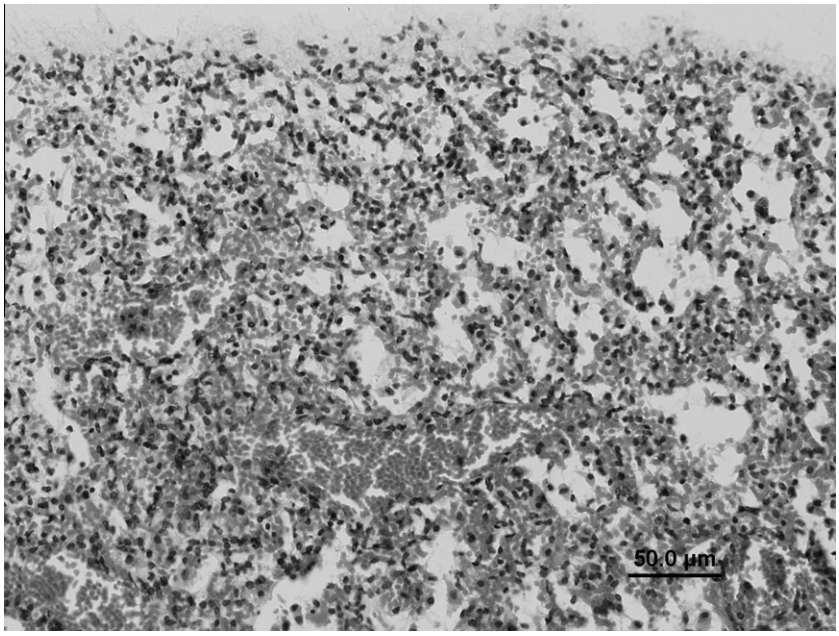

Fig. 3. Lung; *P. multocida*-infected mice (12 h PI). Note scattered hemorrhages and cellular infiltration in the alveolar lumen and thickened inter-alveolar septa. HE; bar = 50 µm.

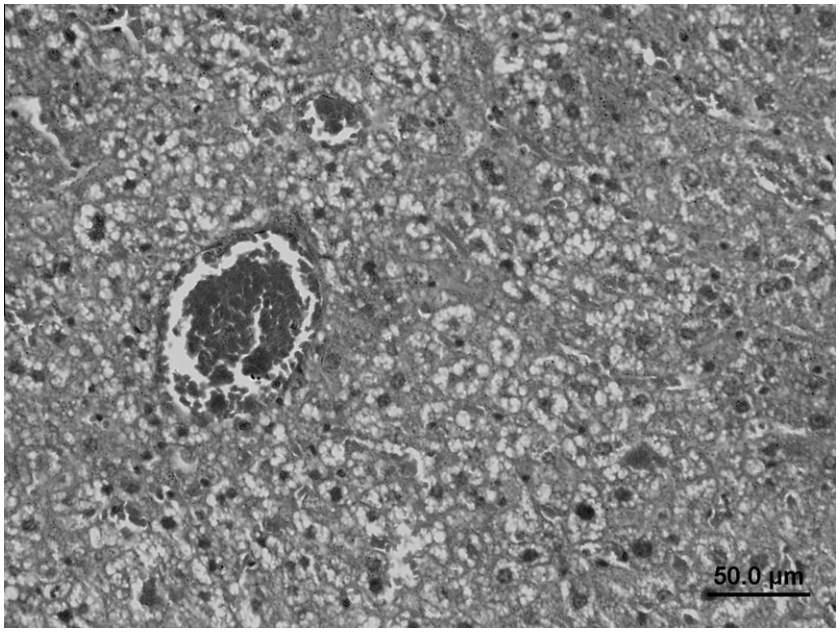

Fig. 4. Liver; *P. multocida*-infected mice (24 h PI). The liver section showing engorged blood vessels and hepatocytes with hydropic degeneration and cytoplasmic vacuolation. HE; bar = 50 µm.

numbers of TUNEL-positive nuclei at white pulp area. A very few numbers of apoptotic nuclei (baseline apoptosis) were observed in tissue sections of control animals.

3.7. Ultrastructural pathology

Lungs showed ultrastructural changes in alveolar epithelium, inter-alveolar septa and capillary endothelium of the lungs. The capillary endothelium was electron-dense and swollen. Pinocytic vesicles and vacuoles were seen in the endothelial cells indicating an acute cell injury (Fig. 6). The type I pneumocytes showed margination of nuclear chromatin and condensation of cytoplasmic matrix, and the damaged type I pneumocytes was lifted from the basal lamina and desquamated into alveolar lumen at places. The type II pneumocytes showed proliferative changes with cytoplasmic vacuolation, and loss of osmiophilic lamellar bodies (Fig. 7). The alveolar macrophages showed a decreased cell density and vacuolations of the rough endoplasmic reticulum. The inter-alveolar septum was thickened and edematous. The capillaries lining inter-alveolar septum were dilated and contained electron-dense plasma and erythrocytes. Alveolar lumen contained neutrophils, desquamated cellular debris and erythrocytes (Fig. 7). The hepatocytes showed swollen mitochondria, dilated endoplasmic reticulum, cytoplasmic vacuoles, and condensed nuclei (Fig. 8).

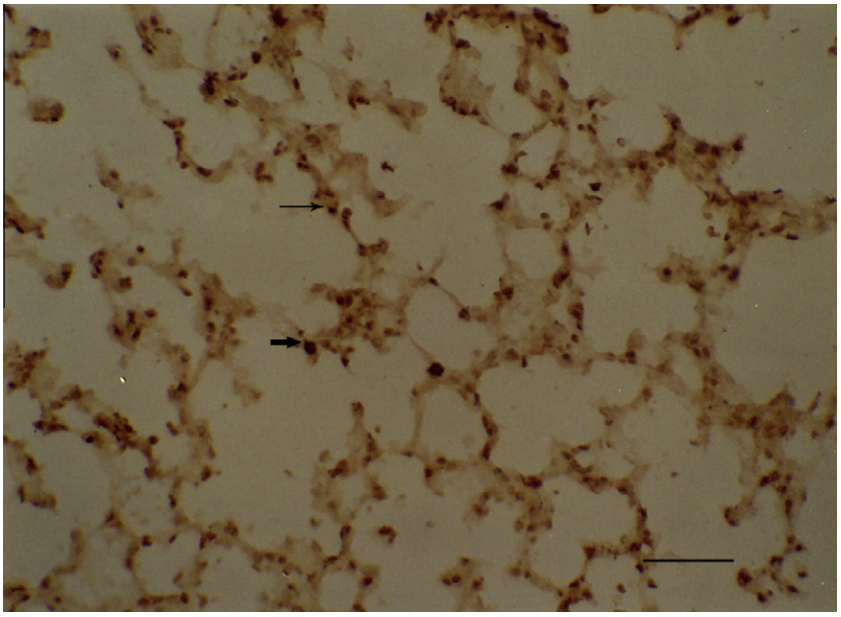

Fig. 5. Lung; *P. multocida*-infected mice (36 h PI). Lung section showing apoptotic nuclei in the alveolar epithelium (thin arrow) and in the infiltrating leukocyte (thick arrow) as dark brown color. Sections were stained by Dead End Colorimetric TUNEL procedure without counter staining. TUNEL; bar = 50 μm.

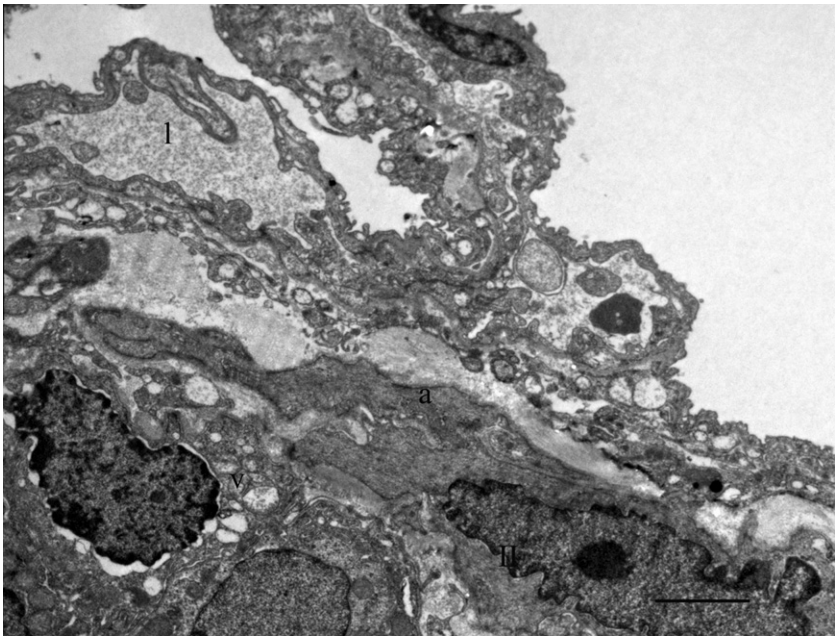

Fig. 6. Lung; *P. multocida*-infected mice (36 h PI). Ultrathin section of lung showing type II pneumocyte with cytoplasmic vacuolation (v) and nuclear chromatin margination. Note loss of osmiophilic lamellar bodies and nuclear bleb formation in other pneumocyte (II). The inter-alveolar septum (a) was thickened and edematous. Note the capillaries lining inter-alveolar septum were dilated and contained electron-dense plasma (l) and reticular structures. Uranyl acetate and lead citrate; bar = 2 μm.

4. Discussion

P. multocida has been associated as a commensal organism in the respiratory tract of mammals and birds, but it is unclear how the bacteria incite acute diseases at times. The current understandings on bacterial interaction with the host suggest that *P. multocida* establishes a complex interaction in host tissues and utilizes available niches effectively to grow rapidly and cause diseases at favourable circumstances (Boyce and Adler, 2006). However, the mechanisms of acute disease pathogenesis and role of bacterial or host factors that induce pathology are poorly understood. The present study was carried out in mice to investigate the serum cytokine profiles, and host cell apoptosis and sequential pathology induced by *P. multocida* serotype A1 at different h PI.

Following infection, animals showed clinical signs of acute infection and few of them were died due to an unrestricted extracellular growth of bacteria resulting in septicemia (Collins, 1973). It was evident from the bacterial isolation made on blood and infected tissues and localization of bacterial antigens or bacterial genome in tissue sections. However, the recovery of low number of viable bacteria and inability to detect bacterial genome at late h PI suggest that bacterial load could be contained by mounting

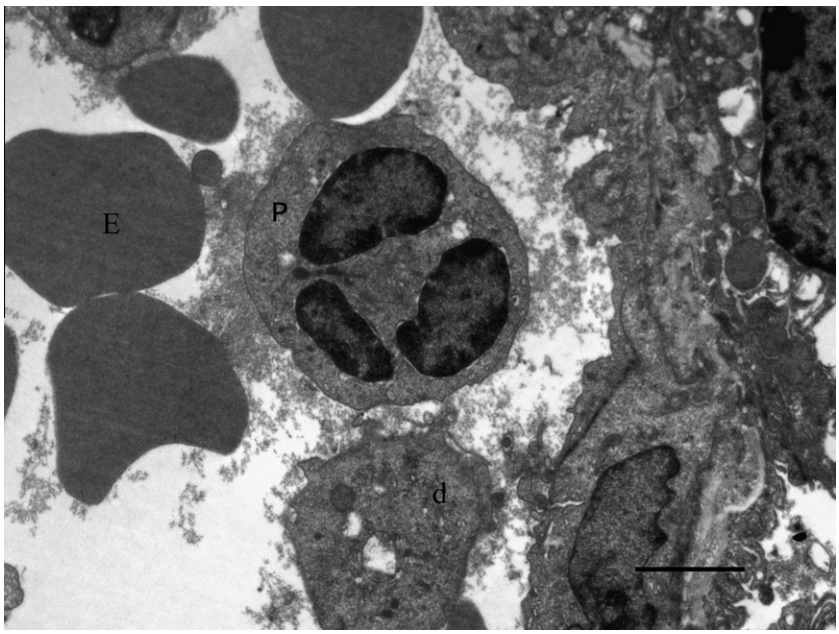

Fig. 7. Lung; *P. multocida*-infected mice (24 h PI). Ultrathin section of lung showing infiltrated polymorphonuclear cell (P) and erythrocytes (E) in the alveolar space. Note desquamated cellular debris (d) near the alveolar wall. Uranyl acetate and lead citrate; bar = 2 μm.

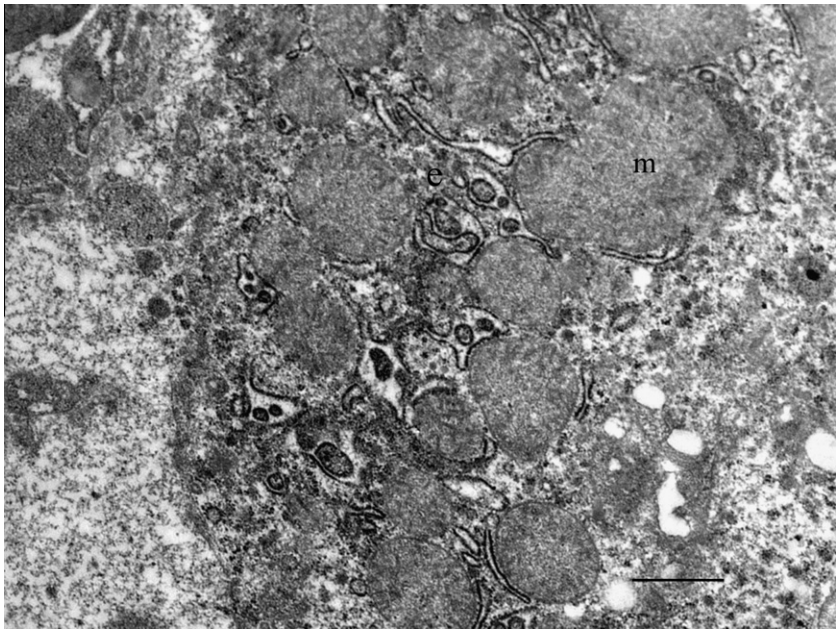

Fig. 8. Liver; *P. multocida*-infected mice (36 h PI). Ultrathin section of liver showing swollen mitochondria (m), dilated endoplasmic reticulum (e), and loss of cytoplasmic contents in the hepatocyte. Uranyl acetate and lead citrate; bar = 1 μm.

immune responses. The observation of reduced lymphocyte counts could be due to drainage of these cells into the tissues or destruction through apoptosis or cytolysis induced by bacterial products (Hotchkiss et al., 1997; Stevens and Czuprynski, 1996; Wesche et al., 2005; Praveena et al., 2007). Analysis of host cell apoptosis revealed that significant numbers of lymphocytes and hepatocytes were apoptotic in the infected mice suggesting that host cells are targeted by bacteria or bacterial toxins as a strategy for initial survival inside the host. Apoptosis of lymphocytes associated with immune dysfunction and mortality had been reported in septicemic mice (Hotchkiss et al., 1997; Wesche et al., 2005). Since humoral and cellular immune responses are involved in containing *P. multocida* infection (Collins, 1977; Ryu and Kim, 2000), bacteria could try to subvert the cellular immune responses of host through induction of apoptosis in immunocompetent cells.

The histological sections of the lungs had PMN cellular infiltration at early and monocytic reaction at late hours of infection. The influx of these cells into the alveolar spaces could be triggered by a surge in pro-inflammatory cytokines (TNF-α, IL-1β, and IL-8) in response to cell wall components of Gram-negative bacteria (Caswell et al., 1998; Locksley et al., 2001; Morrison et al., 1999; Vogel and Hogen, 1990). The LPS and porin proteins isolated from *P. multocida* have been reported to up-regulate the mRNA expression levels of pro-inflammatory cytokines in murine splenic lympho-

cytes (Iovane et al., 1998). The increased serum cytokine levels of pro-inflammatory cytokines at early h PI were correlated with the observation of cellular infiltrates in the lungs and liver. These cytokines were reported to enhance leukocyte transmigration into the site of infection by favouring expression of cell adhesion molecules and production of eicosanoids and prostaglandins that perpetuate the inflammatory cascade in septicemia (Caswell et al., 1998; Morrison et al., 1999; Vogel and Hogen, 1990; Yoshie et al., 2001). The higher levels of these cytokines in blood could also be attributed for fever, anorexia and behavioral changes observed in the infected animals (Locksley et al., 2001; Hodgson, 2006; Vogel and Hogen, 1990).

The chemokine IL-8 or mouse KC is a specific chemotactic factor that activates transmigration of neutrophils into the site of infection (Caswell et al., 1998; Galdiero et al., 2000; Slocombe et al., 1985). The increased level of mouse KC at 12–36 h PI in the present study was directly correlated with more infiltration of PMN cells into the lungs (Caswell et al., 1998; Galdiero et al., 2000; Slocombe et al., 1985). However, IL-6 level was found to be increased after 36 h PI, which coincided with decrease in mouse KC level suggesting that there could be a transition in cytokine profile and inflammatory response at the late hours of infection. It was evident from the observation of increased mononuclear infiltration in the lungs at 60–72 h PI. It has been reported that IL-6 regulates the transition from neutrophil to monocyte recruitment during inflammatory process (Kaplanski et al., 2003). Thus, the bacteria growing in the extracellular milieu could induce cytokine secretion as seen by gradual increase in the levels of pro-inflammatory cytokines in relation to increased viable bacterial counts observed at early h PI. These cytokines further mediate the inflammatory reaction in tissues, while bacteria or bacterial products in association with these cytokines could induce apoptosis of immunocompetent cells.

The ultrastructural and histological changes observed in the lungs and liver resemble an acute cell injury that resulted from the bacterial endotoxins or toxic proteins (Hodgson, 2006; Morrison et al., 1999; Vogel and Hogen, 1990). The histological lesions observed in the lungs were consistent with the findings of previous workers (Okerman et al., 1979; Ramdani et al., 1990). The histology and ultrastructural changes observed in the inter-alveolar septa suggest that the bacteria established septicemia, while the changes such as intra-alveolar exudation and alveolar epithelial changes represent the inflammatory response to bacteria in alveolar airspace. In addition, the presence of cellular exudates in the bronchioles suggests that there was a possible secondary bacterial spread within the lung via airways. The observation of degenerative changes in the liver at early h PI suggests that liver, as an initial organ of bacterial spread from peritoneal cavity, had developed reversible cell injury, which was less pronounced during late h PI. Thus, the bacteria injected in the peritoneal cavity were taken systemically and resulted in septicemia. While establishing systemic infection, bacteria or bacterial products could exploit the host niches (for example, induction of apoptosis in immunocompetent cells or cytokine secretion) for rapid multiplication in the extracellular spaces resulting in severe septicemia. However, the molecular mechanisms by which the bacterial components induce cytokine secretion and host cell apoptosis need to be studied in detail.

In conclusion, a surge in pro-inflammatory cytokines that results in inflammatory reaction in the tissues, and induction of host cell apoptosis were attributed for pathogenesis of pasteurellosis in mice.

Acknowledgements

This study was supported by All India Network projects on Bovine Hemorrhagic Septicemia funded by Indian Council of Agricultural Research. Authors are thankful to the technical staffs in Pathology and Bacteriology departments for their help throughout this study.

References

Boyce, J.D., Adler, B., 2006. How does *Pasteurella multocida* respond to the host environment. Current Opinion in Microbiology 9, 117–122.

Caswell, J.F., Middleton, D.M., Sorden, S.D., Gordon, J.R., 1998. Expression of the neutrophil chemoattractant interlukin-8 in the lesions of bovine pneumonic pasteurellosis. Veterinary Pathology 35, 124–131.

Collins, F.M., 1973. Growth of *Pasteurella multocida* in vaccinated and normal mice. Infection and Immunity 8, 868–875.

Collins, F.M., 1977. Mechanisms of acquired resistance to *Pasteurella multocida* infection – a review. Cornell Veterinarian 67, 103–136.

Fuller, T.E., Kennedy, M.J., Lowery, D.E., 2000. Identification of *Pasteurella multocida* virulence genes in a septicemic mouse model using signature-tagged mutagenesis. Microbial Pathogenesis 29, 25–38.

Galdiero, M., Folgore, A., Nuzzo, I., Galdiero, E., 2000. Neutrophil adhesion and transmigration through bovine endothelial cells *in vitro* by protein H and LPS of *Pasteurella multocida*. Immunobiology 202, 226–238.

Gautam, R., Kumar, A.A., Singh, V.P., Singh, V.P., Dutta, T.K., Shivchandra, S.B., 2004. Specific identification of *Pasteurella multocida* serogroup A-isolates by PCR. Research in Veterinary Science 76, 179–185.

Hodgson, J.C., 2006. Endotoxin and mammalian host responses during experimental disease. Journal of Comparative Pathology 135, 157–175.

Hotchkiss, R.S., Swanson, P.E., Cobb, J.P., Jacobson, A., Buchman, T.G., Karl, I.E., 1997. Apoptosis in lymphoid and parenchymal cells during sepsis: findings in normal and T-and B cell-deficient mice. Critical Care Medicine 25, 1298–1307.

Iovane, G., Paginini, P., Galdiero, M., Cipollaro de l'Ero, G., Vitiello, M., D'Isanto, M., Marcatili, A., 1998. Role of *Pasteurella multocida* porin on cytokine expression and release by murine splenocytes. Veterinary Immunology and Immunopathology 66, 391–404.

Kaplanski, G., Marin, V., Montero-Julian, F., Mantovani, A., Farnarier, C., 2003. IL-6: a regulator of the transition from neutrophil to monocyte recruitment during inflammation. Trends in Immunology 24, 25–29.

Locksley, R.M., Kilken, N., Lenardo, M.J., 2001. The TNF and TNF receptor superfamilies-integrating mammalian biology. Cell 104, 487–501.

Morrison, D.C., Silverstein, R., Lucli, M., Shanrya, A., 1999. Structure–function relationships of bacterial endotoxins-contribution to microbial sepsis. Infectious Disease Clinics of North America 13, 313–340.

Okerman, L., Spanoghe, L., De Bruycker, R.M., 1979. Experimental infection of mice with *Pasteurella multocida* isolated from rabbits. Journal of Comparative Pathology 89, 51–55.

Praveena, P.E., Singh, N., Periasamy, S., Kumar, A.A., 2007. Studies on haematobiochemical changes in *Pasteurella multocida* serotype A1 infection in mice. Indian Journal of Veterinary Pathology 31, 34–36.

Ramdani, C., Dawkins, H.J.S., Johnson, R.B., Spencer, T.L., Adler, B., 1990. *Pasteurella multocida* infections in mice with reference to haemorrhagic septicaemia in cattle and buffalo. Immunology and Cell Biology 68, 57–61.

Ryu, H.I., Kim, C.J., 2000. Immunologic reactivity of a lipopolysaccharide–protein complex of type A *Pasteurella multocida* in mice. Journal of Veterinary Science 1, 87–95.

Slocombe, R.F., Mulks, M., Killingsworth, C.R., Derksen, F.J., Robinson, N.E., 1985. Importance of neutrophils in the pathogenesis of acute pneumonic pasteurellosis in calves. American Journal of Veterinary Research 46, 2253–2258.

Stevens, P.K., Czuprynski, C.J., 1996. *Pasteurella haemolytica* leucotoxin induces bovine leucocytes to undergo morphologic changes consistent with apoptosis in vitro. Infection and Immunity 64, 2687–2694.

Vogel, S.N., Hogen, M.M., 1990. Role of cytokines in endotoxin-mediated host responses. In: Oppenheim, J.J., Shevach, E.M. (Eds.), Immunophysiology – the role of cells and cytokines in immunity and inflammation. Oxford University Press, pp. 238–258.

Wesche, D.E., Lomas-Neira, J.L., Perl, M., Chung, C., Ayala, A., 2005. Leukocyte apoptosis and its significance in sepsis and shock. Journal of Leukocyte Biology 78, 325–337.

Yoshie, O., Imai, T., Nomiyana, H., 2001. Chemokines in immunity. Advances in Immunology 78, 57–110.